

## A multi-phase model for predicting the effective chloride migration coefficient of ITZ in cement-based materials

C.C. Yang<sup>\*2</sup> and S.H. Weng<sup>1a</sup>

<sup>1</sup>Institute of Materials Engineering, National Taiwan Ocean University

<sup>2</sup>Pei-Ning Road, Keelung, Taiwan, 20224, ROC

(Received November 23, 2012, Revised February 25, 2013, Accepted April 18, 2013)

**Abstract.** Mortar microstructure is considered as a three-phase composite material, which is cement paste, fine aggregate and interfacial transition zone. Interfacial transition zone is the weakest link between the cement paste and fine aggregate, so it has a significant role to determine the properties of cementitious composites. In this study, specimens (w/c = 0.35, 0.45, 0.55) with various volume fractions of fine aggregate ( $V_f = 0, 0.1, 0.2, 0.3$  and  $0.4$ ) were cast and tested. To predict the equivalent migration coefficient ( $M_e$ ) and migration coefficient of interfacial transition zone ( $M_{itz}$ ), double-inclusion method and Mori-Tanaka theory were used to estimate. There are two stages to estimate and calculate the thickness of interfacial transition zone ( $h$ ) and migration coefficient of interfacial transition zone ( $M_{itz}$ ). The first stage, the data of experimental chloride ion migration coefficient ( $M_s$ ) was used to calculate the equivalent migration coefficient of fine aggregate with interfacial transition zone ( $M_e$ ) by Mori-Tanaka theory. The second stage, the thickness of interfacial transition zone ( $h$ ) and migration coefficient of interfacial transition zone ( $M_{itz}$ ) was calculated by Hori and Nemat-Nasser's double inclusion model. Between the theoretical and experimental data a comparison was conducted to investigate the behavior of interfacial transition zone in mortar and the effect of interfacial transition zone on the chloride migration coefficient, the results indicated that the numerical simulations is derived to the  $M_{itz}/M_m$  ratio is 2.11~8.28. Additionally, thickness of interfacial transition zone is predicted from  $10 \mu\text{m}$ ,  $60$  to  $80 \mu\text{m}$ ,  $70$  to  $100 \mu\text{m}$  and  $90$  to  $130 \mu\text{m}$  for SM30, M35, M45 and M55, respectively.

**Keywords:** interfacial transition zone; double-inclusion method; Mori-Tanaka theory; migration coefficient of mortar

### 1. Introduction

One of the major deterioration problems of concrete structures to threat the concrete durability and cause corrosion of reinforced steel is chloride ion; especial structures are in deicing salts conditions or coastal marine environments. For diffusivity ability of concrete, it is regarded as significant index that observes the service life of reinforced concrete structures (Martin-Perez *et al.* 2003). Meijers *et al.* (2001) described that complicating of the ingress of chloride ions is caused by the different influencing factors and transport mechanisms, such as heat, moisture and chloride

---

\*Corresponding author, Professor, E-mail: ccyang@mail.ntou.edu.tw

<sup>1a</sup>Ph.D., E-mail: hannahgirl1102@gmail.com

ions transport. Meijers *et al.* (2001) also developed a finite element model by three coupled equations. To investigate chloride diffusion into concrete, the effect of w/c ratio, hydration degree, volume fraction of aggregate, distributing of aggregate particle size, thickness of interfacial transition zone, and air content have to be considered. Parrot and Killoh (1984) described that the hydration of cement particles influenced hydration degree of ITZ and matrix, and developed a model by hydration process and reaction rates. Bentz *et al.* (1998) pointed out the three chief influences on the concrete diffusivity, which were w/c ratio, hydration degree, and volume fraction of aggregate. Shah (2000) also explained that four effects to influence the hydrated cement paste by various aggregate content, which were dilution, tortuosity, interfacial transition zone (ITZ) and percolation effects. Yang and Su (2002) used accelerated chloride migration test (ACMT) to regress analysis and estimate the chloride migration coefficient of mortar at various aggregate content, then obtained the approximate chloride migration coefficient of interfacial transition zone ( $M_{itz}$ ). From above-mentioned references, degree of chloride penetration was a key parameter to predict the influence of individual components of the cement-based materials for concrete structures.

In the mortar, the sand particles are surrounded by hydrated matrix, and the interfacial layer of sand particles has various microstructures whose layer has higher concentration of calcium hydroxide crystals (CH), of errtingite and an increased porosity (Simeonov and Ahmad 1995) than bulk matrix. Thus, the interfacial layer that surrounds the sand particles is called interfacial transition zone (ITZ). Mortar microstructure is delineated by a three-phase composite sphere assemblage, which is cement paste, fine aggregate and ITZ (Dridi 2013). Asbridge *et al.* (2002) obtained that the ITZ is more porous than the bulk matrix at lower water/binder ratios in Portland cement specimens, and the microhardness of the ITZ is 22% and 18% lower than the bulk matrix at a water/binder ratio of 0.4 and 0.5, respectively. Lyubimova and Pinus (1962) estimated microhardness gradients from aggregate to ITZ and cement paste, the result of micro-hardness is derived decreased within 100  $\mu m$  from the aggregate surface. Therefore, some researchers pointed out the ITZ are the weakest link between the cement paste and aggregate, so it has a significant role to determine the properties of all cementitious composites (Ulrik Nilsson and Monteiro 1993, Akçaoğlu *et al.* 2004, 2005).

In the study of ITZ, Bentur and Alexandder (2000), described that factor of engineering properties of cementitious materials influenced the thickness the existence of ITZ. This weak faces of ITZ, which deeply affects the characteristics of mortar such as strength, permeability and durability, must be considered in the three-phase modeling of mortar to capture more realistic behavior of mortar (Lee and Park 2008). In this paper, to consider the three-phase modeling (cement paste, ITZ and fine aggregate) of mortar and predict the equivalent migration coefficient ( $M_e$ ) and migration coefficient of ITZ ( $M_{itz}$ ), double-inclusion method (Nemat-Nasser and Hori 1993) and Mori-Tanaka theory (Mori and Tanaka 1973, Yang 1998) were used to estimate; Between the theoretical and experimental data a comparison was conducted.

## 2. Experimental program

In this study, specimens were made of ASTM Type I Portland cement, water, and fine aggregate. The fine aggregate passing the No. 3/8" sieve and retained on No. #100 was used. For mixes, the water/cement ratio is 0.35, 0.45 and 0.55, respectively. In order to investigate the effect

Table 1 Mix design and volume fraction of aggregate

Mix	Water	Cement	Sand	$V_f^*$
	(kg/m <sup>3</sup> )	(kg/m <sup>3</sup> )	(kg/m <sup>3</sup> )	
M35-0	513.9	1468.3	0	0
M35-1	461.5	1318.4	269.0	0.1
M35-2	409.0	1168.6	538.0	0.2
M35-3	356.6	1018.8	807.0	0.3
M35-4	304.2	869.0	1076.9	0.4
M45-0	574.6	1276.9	0	0
M45-1	516.0	1146.6	269.0	0.1
M45-2	457.4	1016.3	538.0	0.2
M45-3	398.7	886.0	807.0	0.3
M45-4	340.1	755.7	1076.9	0.4
M55-0	621.4	1129.7	0	0
M55-1	558.0	1014.5	269.0	0.1
M55-2	494.5	899.2	538.0	0.2
M55-3	431.1	783.9	807.0	0.3
M55-4	367.7	668.6	1076.9	0.4

\*Volume fraction of aggregate ( $V_f$ ) = volume of fine aggregate / mortar

Table 2 Densities of the constituent materials (g/cm<sup>3</sup>)

Water	Cement	Normal Sand
1	3.15	2.69

Table 3 Fine aggregate sieve analysis

Fine aggregate sieve analysis						
Sieve No.	Aggregate diameter (mm)	Avg. aggregate diameter(mm)	Retained (g)	Retained (%)	Cumulative retained (%)	Cumulative passing (%)
3/8"	9.50		0	0	0	100
No.4	4.75		1.480	0.0148	1.280	98.72
No.8	2.36		24.01	0.2401	25.02	74.98
No.16	1.18	1.56	29.36	0.2936	53.74	46.26
No.30	0.60		22.20	0.2220	76.12	23.88
No.50	0.30		19.30	0.1930	96.32	3.680
No.100	0.15		0.060	0.0006	96.38	3.620
Cumulative	--	--	18.1	3.62	100	0

of the chloride migration coefficient of mortar at various volume fractions of fine aggregate (the volume of fine aggregate/ the volume of mortar,  $V_f$ ), the range is selected from 0% to 40%. The proportion of the mixtures listed in Table 1. The densities of the constituent materials and fine aggregate sieve analysis are listed in Table 2 and Table 3. Each cylindrical specimen ( $\phi 100 \times 200$

mm) was cast and cured; the specimen (30 mm in thickness) was taken from the middle part of the cylindrical specimen. Accelerated chloride migration test (ACMT) was developed to measure and obtain the concentration of cumulative chloride ions passing through the specimen under 24 voltages (Yang 2003, Yang and Liang 2009). Before Accelerated chloride migration test (ACMT), the specimens were prepared and followed the specification in ASTM C1202-97.

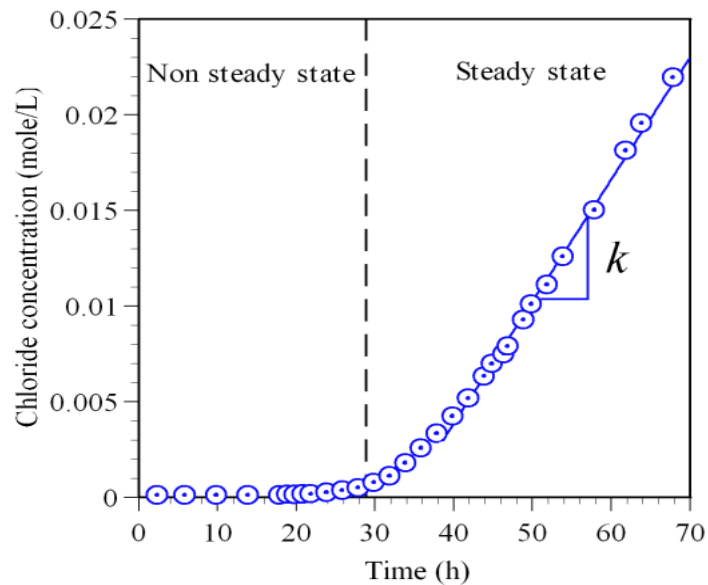


Fig. 1 The typical result of chloride concentration as a function of time

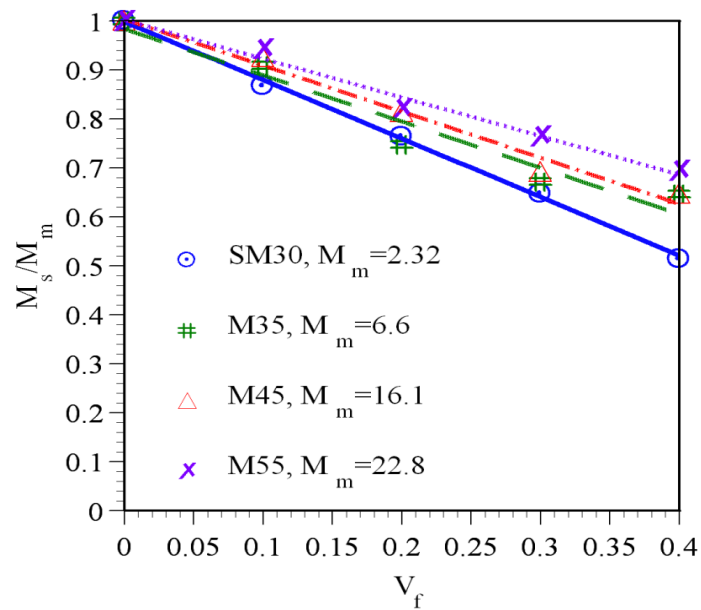


Fig. 2 The numerical chloride migration coefficient of mortar

### 3. Results and discussion

#### 3.1 Chloride migration coefficient

The chloride concentration was measured and determined from the solution in the anodic cell of ACMT, there were four stages which are non-steady state, transition period, steady state, and attenuate (Yang 2003). The typical result of chloride concentration is plotted as a function of time in Fig. 1. The steady state stage is obtained from the linear regression when the optimal correlation coefficient ( $R^2 \approx 1$ ) of the linear line was determined by using trial and error method. For chloride ion penetration, the chloride migration rate ( $k$ ) is calculated as (Yang and Liang 2009)

$$C = kt + b \quad (1)$$

where  $C$  is the chloride concentration (mole/L),  $k$  (chloride migration rate) is the slope of the chloride–time curve (mole/L $\times$ h $^{-1}$ ),  $b$  is a type of constant. Using the Nernst–Planck's equation, the steady state migration coefficient,  $M_s$  (cm $^2$ /s), is calculated as (Andrade 1993, Yang and Liang 2009):

$$M_s = \frac{RTL}{|z|C_0FE} \frac{kV}{A} \quad (2)$$

where  $R$  is universal gas constant ( $R = 8.314 \text{ J/K} \times \text{mole}^{-1}$ ),  $T$  is absolute temperature ( $K$ ),  $L$  is the thickness of specimen (m),  $z$  is valence electron of chloride ion,  $C_0$  is initial chloride concentration in cathode cell (mole/L),  $F$  is Faraday constant ( $F = 96500 \text{ J/V} \times \text{mole}^{-1}$ )  $E$  is applied voltage (V),  $V$  is the volume of solution in anodic cell (m $^3$ ), and  $A$  is the specimen surface exposed to chloride ions (m $^2$ ). In this study, using the chloride migration rate ( $k$ , Eq. (1)) and Nernst–Planck's equation, the steady state migration coefficient ( $M_s$ , Eq. (2)) is obtained and applied to investigate and determine the relationship of migration coefficient with various volume fractions of fine aggregate (Andrade 1993, Yang 2003, Yang and Liang 2009), all specimens are calculated and listed in Table 4.

In this study, the average diameter of fine aggregate particles is assumed as spherical. The average diameter of fine aggregate is 1.557 mm (in Table 3). The average of steady state migration coefficient of cement paste obtained from experimental result as shown in Table 4,  $M_m$ , is  $6.6 \times 10^{-8}$ ,  $16.1 \times 10^{-8}$  and  $22.8 \times 10^{-8}$  (cm $^2$ /s) for series M35, M45 and M55, respectively.

In order to compare the discrepancy of sand diameter and adding mineral admixture, a series of experimental results (SM30) were used as a reference (Cho 2002), in which that specimens were made of ASTM Type I Portland cement, water and Ottawa sand (the average diameter was  $350 \mu\text{m}$ ); water/binder ratio of specimen was 0.3 with 10% silica fume; and the volume fraction of Ottawa sand was designed from 0% to 40%. The specimens were cured in water (23°C) for 91 days, and were followed the specification in ASTM C1202-97 and prepared to the accelerated chloride migration test (ACMT). The experimental result (SM30) (Cho 2002) indicated that the steady state migration coefficient of cement paste,  $M_m$ , is  $2.32 \times 10^{-8}$  (cm $^2$ /s) for w/b ratio of 0.3 (see in Table 4).

As showing in Fig. 2, the steady state migration coefficient of mortar is normalized by the migration coefficient of paste, and the normalized migration coefficient decreases with an increase in volume fraction of fine aggregate. The slope of experimental result decreases with a decrease in

Table 4 The steady-state migration coefficient (M35, M45, M55 and SM30)

$V_f$	M35		M45		M55		SM30 (Cho 2002)	
	$M_s$ ( $\times 10^{-8}$ cm <sup>2</sup> /s)	$\frac{M_s}{M_m}$	$M_s$ ( $\times 10^{-8}$ cm <sup>2</sup> /s)	$\frac{M_s}{M_m}$	$M_s$ ( $\times 10^{-8}$ cm <sup>2</sup> /s)	$\frac{M_s}{M_m}$	$M_s$ ( $\times 10^{-8}$ cm <sup>2</sup> /s)	$\frac{M_s}{M_m}$
0	6.6		16.1		22.8			
	6.4	1	15.6	1	23.5	1	2.32	1
	6.7		16.6		22.1			
0.1	5.9	0.894	14.7	0.913	21.2	0.930		
	6	0.909	14.9	0.925	21.8	0.956	2.01	0.866
	6.1	0.924	15.1	0.938	21.5	0.943		
0.2	5.1	0.773	13.2	0.820	19.8	0.868		
	4.9	0.742	13.5	0.839	18.8	0.825	1.77	0.763
	4.8	0.727	12.6	0.783	17.5	0.768		
0.3	4.3	0.652	11.1	0.689	17.2	0.754		
	4.6	0.697	11.4	0.708	17.7	0.776	1.5	0.647
	4.4	0.667	10.9	0.677	17.4	0.763		
0.4	4.1	0.621	10.3	0.640	17.5	0.768		
	4.2	0.636	10.4	0.646	14.5	0.636	1.19	0.513
	4.5	0.682	10.5	0.652	15.5	0.680		

w/c ratios, the mortar quality of SM30 is greater than M35, M45 and M55. Because SM30 has lower w/b ratio with 10% silica fume, the discontinued pores of cement particles were gradually filled with mineral admixtures and hydration products.

### 3.2 Effect of volume fraction of aggregate

Shah (2000) indicated that the influence of aggregate in the hydrated cement paste is dilution, tortuosity, ITZ, and percolation effects. For the dilution effect, in the ACMT, the route of chloride ions migration is blocked by aggregate (Yang 2003, Yang and Liang 2009), the chloride migration coefficient of mortar,  $M$ , can be expressed as (Shah 2000, Yang and Su 2002)

$$M = M_m(1 - V_f) + M_a V_f \quad (3)$$

where  $V_f$  is volume fractions of fine aggregate, the aggregate is relatively impermeable to cement paste, the migration coefficient of fine aggregate ( $M_a$ ) is considered to assume zero. Therefore, Eq. (3) is expressed as Eq. (4)

$$M = M_m(1 - V_f) \quad (4)$$

Moreover, for tortuosity effect, route of chloride ions migration is compelled to detour around the aggregate particles, so reduced the rate of chloride ions migration. By combining the tortuosity

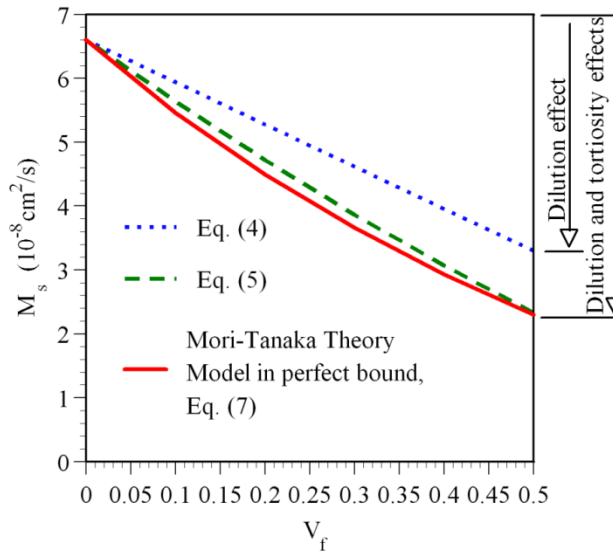


Fig. 3 Theoretical results of Migration coefficient of mortar with perfect bound

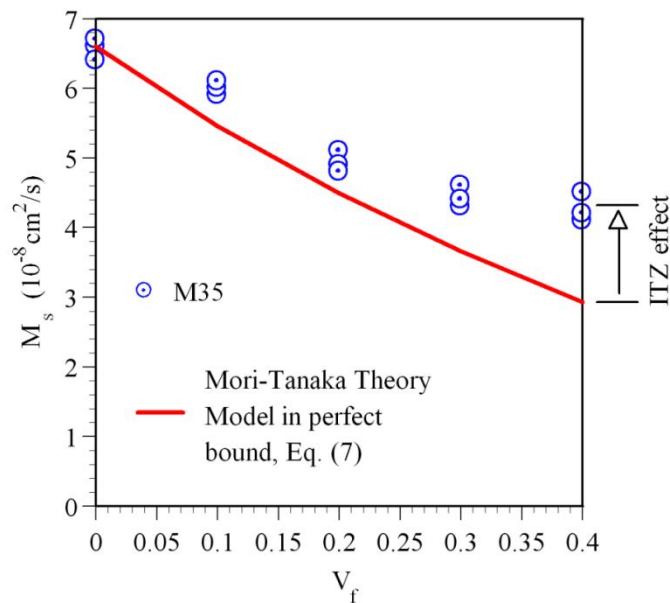


Fig. 4 The relationship between the numerical simulations of Mori-Tanaka theory model with perfect bound and chloride migration coefficient of M35

effect with the dilution effect, the chloride migration coefficient of mortar can be expressed by the Bruggeman equation, as follows (Bruggeman 1935)

$$M = M_m (1 - V_f)^{1.5} \tag{5}$$

By Mori-Tanaka theory, to calculate the overall average migration coefficient of two-phase composite materials,  $M_c$ , is provided as follow (Mori and Tanaka 1973, Yang 1998)

$$M_c = \left\{ M_m^{-1} + V_f \left[ \left( (1 - V_f)(M_a - M_m)S - V_f(M_m - M_a) + M_m \right)^{-1} \right] (M_m - M_a) M_m^{-1} \right\}^{-1} \quad (6)$$

where  $M_a$  is the migration coefficient of aggregate,  $S$  is the component  $S_{1111}$  of the Eshelby tensor for a single inclusion. In the theoretical result of viewpoint, the migration coefficient of mortar is regarded as lower than migration coefficient of cement pastes if the bond between fine aggregate and cement paste is a perfect bound. Therefore, for the theoretical model with perfect bound, which indicate that the cement-based material is a two-phase composite material, and the  $M_a$  is regarded as zero, the Eq. (6) is expressed as Eq. (7)

$$M_c = \frac{M_m(1 - V_f)(1 - S)}{S(V_f - 1) + 1} \quad (7)$$

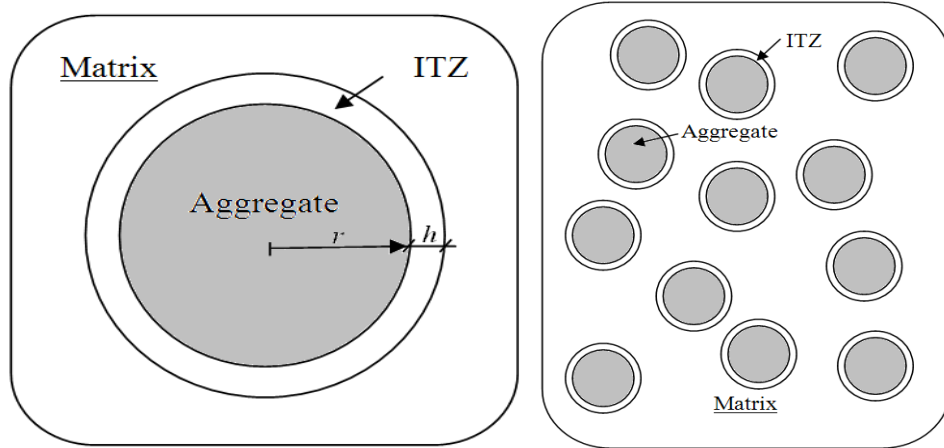
In Table 5 and Fig. 3, to predict theoretical results of mortar migration coefficient (M35,  $M_m = 6.6 \times 10^{-8} \text{ cm}^2/\text{s}$ ) with perfect bound, the chloride migration coefficient of mortar is plotted varied with increased the volume fraction of fine aggregate, and theoretical results of three curves are compared in Eqs. (4), (5) and (7).

For ability of resistible chloride ion penetration, the dilution and the tortuosity effects are positive. In the Fig. 3, the Mori-Tanaka theory model with perfect bound (Eq. (7)) is close to the Bruggeman equation (Eq. (5)), it being the case that the Mori-Tanaka theory model with perfect bound is replaced as lower bound, then further step is applied to predict the numerical simulations of migration coefficient of mortar.

Relative to the ITZ and percolation effects, it is negative effects to resist penetration of chloride ion. In Fig. 4, comparing the experimental results (M35,  $M_m = 6.6 \times 10^{-8} \text{ cm}^2/\text{s}$ ) and numerical simulations of Mori-Tanaka theory model with perfect bound (Eq. (7)), chloride migration coefficient of mortar (M35) are higher than Mori-Tanaka theory model with perfect bound (Eq. (7)); the difference between the numerical simulations of Mori-Tanaka theory model with perfect bound and experimental results are increased with increased volume fraction of fine aggregate. It means the ITZ may have occurred. Thus, it is reasonable to consider the third phase (ITZ) in the analytical prediction.

Table 5 Theoretical results of mortar migration coefficient with perfect bound ( $M_c \times 10^{-8} \text{ cm}^2/\text{s}$ )

$V_f$	$M = M_m(1 - V_f)$ Eq. (4)	$M = M_m(1 - V_f)^{1.5}$ Eq. (5)	Mori-Tanaka theory model with perfect bound Eq. (7)
0	6.60	6.60	6.60
0.1	5.94	5.64	5.46
0.2	5.28	4.72	4.49
0.3	4.62	3.87	3.66
0.4	3.96	3.07	2.93
0.5	3.30	2.33	2.30



(a) aggregate particles with ITZ in matrix (b) Aggregate and ITZ in Matrix

Fig. 5 The model of three-phase composite materials of mortar

### 3.3 Equivalent migration coefficient in double-inclusion method

Mortar microstructure is delineated by an assemblage of three-phase composite materials, which is cement paste, ITZ and fine aggregate (Dridi 2013). In this study, the equivalent of spherical shape was considered in a model, fine aggregate was regards as an inclusion, the ITZ was regards as another inclusion that a uniform layer around the aggregate (see in Fig. 5(a)). In addition, these equivalents of spherical shape were not overlapped to be embedded in an infinite matrix randomly (see in Fig. 5(b))(Yang 1998).

Young's modulus of concrete was deemed as resemblance to equation of chloride migration coefficient, for instance,  $M \equiv E$  ( $E$  is the Young's modulus of concrete),  $J \equiv \sigma$  ( $\sigma$  is the applied stress), and  $\frac{\partial Cl}{\partial x} \equiv \varepsilon$  ( $\varepsilon$  is the induced strain)(Hobbs 1999). The models result in the following solutions for migration coefficient of mortar ( $M$ ). Chloride migration that occurs in the cement paste matrix can be described by using the migration equation, as follows

$$J = M \frac{\partial Cl}{\partial x} \quad (8)$$

Therefore, Young's modulus and double-inclusion method was applied to the same concept by chloride migration coefficient in this study. Matrix with infinite large body which has migration coefficient of cement paste ( $M_m$ ) is assumed contain two inclusions, one inclusion is the migration coefficient of fine aggregate ( $M_a$ ); another inclusion is migration coefficient of ITZ ( $M_{itz}$ ). When two-phase composite materials (aggregate and ITZ) were considered as similar concentric spheres but different radius, the equivalent migration coefficient of aggregate with ITZ,  $M_e$ , is derived as (Nemat-Nasser and Hori 1993, Yang 1998)

$$M_e = M_m [1 + (S - 1)B] (1 + SB)^{-1} \quad (9)$$

where  $S$  is the component  $S_{1111}$  of the Eshelby tensor for a single inclusion,  $B$  is defined as

$$B = \frac{V_e}{(B_a - S)} + \frac{(1 - V_e)}{(B_{itz} - S)} \quad (9-1)$$

$V_e$  is defined as

$$V_e = \frac{\frac{4}{3}\pi\left(\frac{r}{2}\right)^3}{\frac{4}{3}\pi\left(\frac{r}{2} + h\right)^3} = \frac{\left(\frac{r}{2}\right)^3}{\left(\frac{r}{2} + h\right)^3} \quad (9-2)$$

where  $r$  is radius of fine aggregate,  $h$  is the thickness of ITZ and  $V_e$  is volume fraction of aggregate in equivalent ( $V_e = \text{Volume of fine aggregate} / \text{ITZ with fine aggregate}$ ).  $B_a$  is defined as

$$B_a = M_m (M_m - M_a)^{-1} \quad (9-3)$$

The aggregate is relatively impermeable to cement paste, the migration coefficient of fine aggregate ( $M_a$ ) is consider to assume zero. Therefore, Eqs. (9-3) is expressed as Eq. (9-4)

$$B_a = 1 \quad (9-4)$$

where  $B_{itz}$  are defined as,

$$B_{itz} = M_m (M_m - M_{itz})^{-1} \quad (9-5)$$

To predict the equivalent migration coefficient of aggregate with ITZ ( $M_e$ ), the double-inclusion method (Nemat-Nasser and Hori 1993) is used.

### 3.4 Overall migration coefficient of cement-based materials

By Mori-Tanaka theory, three-phase composite materials of mortar microstructure is applied to estimate the overall migration coefficient of mortar,  $M_c$ , it is provided as follow in Eq. (10) (Mori and Tanaka 1973, Yang 1998).

$$M_c = \left\{ M_m^{-1} + V_f \left[ \left( (1 - V_f)(M_e - M_m)S - V_f(M_m - M_e) + M_m \right)^{-1} \right] (M_m - M_e) M_m^{-1} \right\}^{-1} \quad (10)$$

In this study, there are two main stages to calculate the migration coefficient of three-phase composite materials. The first stage, the data of experimental chloride ion migration coefficient ( $M_s$ ) was used to calculate the equivalent migration coefficient of fine aggregate with interfacial transition zone ( $M_e$ ) by Mori-Tanaka theory. The second stage, the thickness of interfacial transition zone ( $h$ ) and migration coefficient of interfacial transition zone ( $M_{itz}$ ) was calculated by Hori and Nemat-Nasser's double inclusion model.

Figure 6 is the relationship between chloride migration coefficient of mortar and  $V_f$ . For the first stage, the experimental result of chloride ion migration coefficient ( $M_s$ ) was used to curve fitting the equivalent migration coefficient of fine aggregate with ITZ ( $M_e$ ) by Eq. (10) (see in the Fig. 6). The equivalent migration coefficient of fine aggregate with ITZ ( $M_e$ ) is obtained from the

Table 6 The migration coefficient of matrix ( $M_m$ ) and the equivalent migration coefficient of fine aggregate and interfacial transition zone ( $M_e$ ), ( $\times 10^{-8}$  cm<sup>2</sup>/s)

Mix	$M_m$	$M_e$
	Experiment results	Theoretical results
SM30 (Cho)	2.23	0.30
M35	6.6	1.56
M45	16.1	4.52
M55	22.8	8.49

Table 7 The assumed range of thickness of ITZ ( $h$ ) and numerical ITZ migration coefficient ( $M_{itz} / M_m$ )

Mix	$M_m$ ( $\times 10^{-8}$ cm <sup>2</sup> /s)	$M_e$ ( $\times 10^{-8}$ cm <sup>2</sup> /s)	$r$ (cm)	$h$ ( $\mu m$ )	$V_e$	$M_{itz}$ ( $\times 10^{-8}$ cm <sup>2</sup> /s)	$M_{itz} / M_m$
SM30 (Cho, 2000)	2.32	0.30	0.035	10	0.846	5.023	2.16
				60	0.800	45.682	6.92
M35	6.6	1.56	0.156	70	0.772	22.963	3.48
				80	0.746	15.574	2.36
				70	0.772	120.069	7.46
M45	16.1	4.52	0.156	80	0.746	63.768	3.96
				90	0.720	44.053	2.74
				100	0.696	34.011	2.11
				90	0.720	188.839	8.28
M55	22.8	8.49	0.156	100	0.696	109.945	4.82
				110	0.673	78.578	3.45
				120	0.650	61.739	2.71
				130	0.629	51.238	2.25

regression analysis and listed in Table 6. The experimental result delineate that the migration coefficient of mortar decreases with an increase in volume fraction of fine aggregate. For w/b = 0.3 (SM30), this experimental results of the mortar migration coefficient is under other mixes (M35, M45 and M55) because this test data (SM30) have lower w/b ratio with 10% silica fume. With the progress of hydration and the discontinued pores of cement particles will be gradually filled with mineral admixtures and hydration products varies with time, caused improving the quality of ITZ. The average result for chloride migration coefficient of cement paste ( $M_m$ ) is listed in the Table 6.

For the second stage,  $B$  is carried out from the first stage of equivalent migration coefficient of fine aggregate with ITZ ( $M_e$ ) by Eq. (9). The ranges of thickness of ITZ ( $h$ ) is assumed as 0~130  $\mu m$ , and the  $V_e$ ,  $B_{itz}$  and  $M_{itz}$  are calculated from Eqs. (9-2), (9-1) and (9-5), respectively. In this study, the numerical ITZ migration coefficient ( $M_{itz} / M_m$ ) is applied to analyze the possible range of the ITZ ( $h$ ) thickness for SM30, M35, M45 and M55. Moreover, the equivalent migration coefficient ( $M_e$ ) is obtained from experimental result, the  $M_{itz} / M_m$  ratio is considered as positive definite and the range between 2~10. Because the  $M_{itz} / M_m$  ratio is over high, the quality of ITZ properties compare with cement paste is exceedingly porous and cavernous. Also, if the  $M_{itz} / M_m$  ratio is lower than double, which means that the quality of ITZ properties is almost equal to cement paste properties or better than cement paste properties. Table 7 is the assumed range of thickness of ITZ ( $h$ ) and the numerical ITZ migration coefficient ( $M_{itz} / M_m$ ).

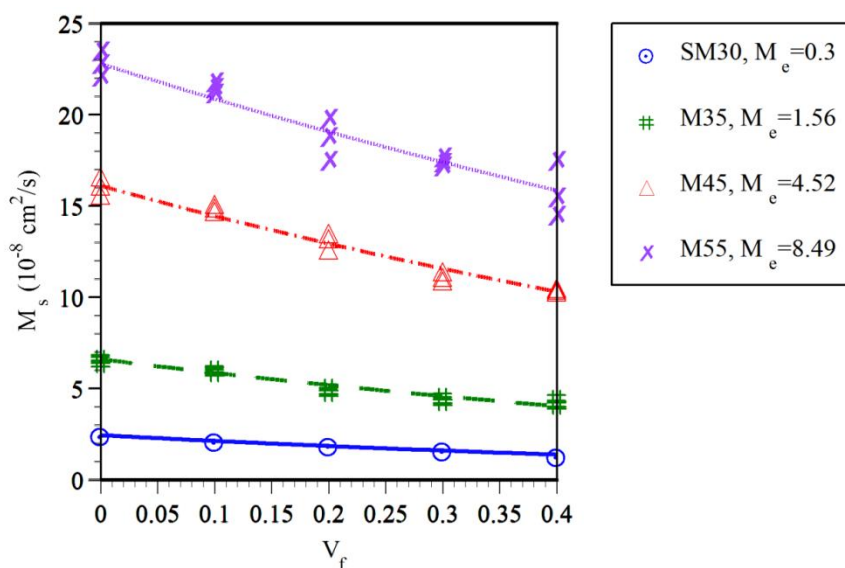


Fig. 6 The relationship between chloride migration coefficient of mortar and  $V_f$

For the second stage,  $B$  is carried out from the first stage of equivalent migration coefficient of fine aggregate with ITZ ( $M_e$ ) by Eq. (9). The ranges of thickness of ITZ ( $h$ ) is assumed as 0~130  $\mu\text{m}$ , and the  $V_e$ ,  $B_{itz}$  and  $M_{itz}$  are calculated from Eqs. (9-2), (9-1) and (9-5), respectively. In this study, the numerical ITZ migration coefficient ( $M_{itz}/M_m$ ) is applied to analyze the possible range of the ITZ ( $h$ ) thickness for SM30, M35, M45 and M55. Moreover, the equivalent migration coefficient ( $M_e$ ) is obtained from experimental result, the  $M_{itz}/M_m$  ratio is considered as positive definite and the range between 2~10. Because the  $M_{itz}/M_m$  ratio is over high, the quality of ITZ properties compare with cement paste is exceedingly porous and cavernous. Also, if the  $M_{itz}/M_m$  ratio is lower than double, which means that the quality of ITZ properties is almost equal to cement paste properties or better than cement paste properties. Table 7 is the assumed range of thickness of ITZ ( $h$ ) and the numerical ITZ migration coefficient ( $M_{itz}/M_m$ ).

For the M35, the 50  $\mu\text{m}$  thickness of ITZ or thinner than 50  $\mu\text{m}$  is assumed, then the  $M_{itz}/M_m$  ratio is minus. When 60  $\mu\text{m}$  thickness of ITZ is assumed, the experimental result of migration coefficient ( $M_s$ ) is closest the curves of numerical simulations which  $M_{itz}/M_m$  ratios 6.92; When 70  $\mu\text{m}$  thickness of ITZ is assumed, the  $M_{itz}/M_m$  ratios 3.48; When 80  $\mu\text{m}$  thickness of ITZ is assumed, the  $M_{itz}/M_m$  ratios 2.36; When 130  $\mu\text{m}$  thickness of ITZ is assumed, the  $M_{itz}/M_m$  ratio is 0.98. That means the quality of ITZ properties is better than cement paste properties, it is not reasonable for ITZ properties. Therefore, when 60~80  $\mu\text{m}$  thickness of ITZ is assumed, the migration coefficient of experimental result (M35) is closest the curves of numerical simulations which  $M_{itz}/M_m$  ratio is from 2.36 to 6.92.

For the M45, when 70 ~ 100  $\mu\text{m}$  thickness of ITZ is assumed, the  $M_{itz}/M_m$  ratio is from 2.11 to 7.46. For the M55, when 90 ~ 130  $\mu\text{m}$  thickness of ITZ is assumed, the  $M_{itz}/M_m$  ratio is from 2.25 to 8.28. For the SM30, when 10  $\mu\text{m}$  thickness of ITZ is assumed, the  $M_{itz}/M_m$  ratio is 2.16. Due to the aforementioned numerical simulations and predicted, no matter the result of mortar migration coefficient ( $M_s$ ), thickness of ITZ ( $h$ ) or curves of numerical simulations ( $M_{itz}/M_m$ ), the SM30 (adding mineral admixtures) is lowest and thinnest than the UN-add mineral admixtures

of M35, M45 and M55.

From Hori and Nemat-Nasser's double inclusion model (Eq. (9)), the ITZ thickness is predicted from  $10\ \mu\text{m}$ ,  $60$  to  $80\ \mu\text{m}$ ,  $70$  to  $100\ \mu\text{m}$  and  $90$  to  $130\ \mu\text{m}$  for SM30, M35, M45 and M55, respectively. Additionally, the  $M_{itz}/M_m$  ratio is 2.16, 2.36~6.96, 2.11~7.46 and 2.25~8.28 for SM30, M35, M45 and M55, respectively. From the above discussions, it is conclusive characterizes to influence the chloride migrativity of mortar is the chloride migrativity of ITZ.

#### 4. Conclusions

Degree of chloride penetration was a key parameter to predict the influence of individual components of the cement-based materials for mortar. Results are obtained from the experimental investigation and the following conclusions are offered:

(1) By Hori and Nemat-Nasser's double inclusion model and Mori-Tanaka theory, the thickness of ITZ ( $h$ ) is assumed and migration coefficient of ITZ ( $M_{itz}$ ) could be predicted.

(2) With the progress of hydration and the discontinued pores of cement particles will be gradually filled with mineral admixtures and hydration products varies with time, caused improving the quality of ITZ. The SM30 result (lower w/b with mineral admixtures) of mortar migration coefficient ( $M_s$ ), thickness of ITZ ( $h$ ) and curves of numerical simulations ( $M_{itz}/M_m$ ) are lowest and thinnest than the UN-add mineral admixtures of M35, M45 and M55.

(3) The different between the theoretical result of Mori-Tanaka theory model with perfect bound and experimental results of migration coefficient ( $M_s$ ) are increased with increased volume fraction of fine aggregate.

(4) For w/b=0.3 (SM30), the ratio of  $M_{itz}/M_m$  is 2.16 as a  $10\ \mu\text{m}$  thickness of ITZ is assumed. For w/c=0.35 (M35), the ratio of  $M_{itz}/M_m$  is 2.36~6.92 as a  $60\sim 80\ \mu\text{m}$  thickness of ITZ is assumed; For w/c=0.45 (M45), the ratio of  $M_{itz}/M_m$  is 2.11~7.46 as a  $70\sim 100\ \mu\text{m}$  thickness of ITZ is assumed. For w/c = 0.55 (M55), the ratio of  $M_{itz}/M_m$  is 2.25~8.28 as a  $90\sim 130\ \mu\text{m}$  thickness of ITZ is assumed.

#### Acknowledgments

The financial support of National Science Council, ROC, under the grants NSC 101-2221-E-019-061-MY3 is gratefully appreciated.

#### References

- Akçaoğlu, T., Tokyay, M. and Çelik, T. (2004), "Effect of coarse aggregate size and matrix quality on ITZ and failure behavior of concrete under uniaxial compression", *Cement Concrete Compos.*, **26**(6), 633-638.
- Akçaoğlu, T., Tokyay, M. and Çelik, T. (2005), "Assessing the ITZ microcracking via scanning electron microscope and its effect on the failure behavior of concrete", *Cement Concrete Compos.*, **35**(2), 358-363.
- Andrade, C. (1993), "Calculation of chloride diffusion coefficients in concrete from ionic migration measurements", *Cement Concrete Res.*, **23**(3), 724-742.
- Asbridge, A.H., Page, C.L. and Page, M.M. (2002), "Effects of metakaolin, water/binder ratio and interfacial transition zones on the microhardness of cement mortars", *Cement Concrete Res.*, **32**(9), 1365-1369.
- Bentur, A. and Alexander, M.G.D. (2000), "Review of the work of the RILEM TC 159-ETC: Engineering of

- the interfacial transition zone in cementitious composites”, *Mater. Struct.*, **33**(2), 82-87.
- Bentz, D.P., Garboczi, E.J. and Lagergren, E.S. (1998), “Multi-scale microstructural modeling of concrete diffusivity: identification of significant variables”, *Cement, Concrete Aggregates J.*, **20**(1), 129-139.
- Bruggeman, D.A.G. (1935), “Dielectric constant and conductivity of mixtures of isotropic materials”, *Annal. Phys.*, **24**, 636-679.
- Cho, S.W. (2002), “Study of chloride-ion transport behavior in cement-based composites using accelerated chloride migration test”, Ph.D. Dissertation, National Taiwan Ocean University, Taiwan.
- Dridi, W. (2012), “Analysis of effective diffusivity of cement based materials by multi-scale modelling”, *Mater. Struct.*, **46**(1-2), 313-326.
- Hobbs, D.W. (1999), “Aggregate influence on chloride ion diffusion into concrete”, *Cement Concrete Res.*, **29**, 1995-1998.
- Lee, K.M. and Park, J.H. (2008), “A numerical model for elastic modulus of concrete considering interfacial transition zone”, *Cement Concrete Res.*, **38**(3), 396-402.
- Lyubimova, T.Y. and Pinus, E.R. (1962), “Crystallization structure in the contact zone between aggregate and cement”, *Concr. Kolloidn. Z. (USSR)*, **24**(5), 578-587.
- Martin-Perez, B., Lounis, Z. and Naus, D.J. (2003), “Numerical modelling of service life of reinforced concrete structures”, *Actas del 2nd International RILEM Workshop of Life Prediction and Aging Management of Concrete Structures*, Paris, France, May.
- Meijers, S.J.H., Bijen, J.M.J.M., De Borst, R. and Fraaij, A.L.A. (2001), “Computational modelling of chloride ion transport in reinforced concrete”, *Heron*, **46**(3), 207-216.
- Mori, T. and Tanaka, K. (1973), “Average stress in matrix and average elastic energy of materials with misfitting inclusions”, *Acta Metallurgica*, **21**(5), 571-574.
- Nemat-Nasser, S. and Hori, M. (1993), *Overall properties of Heterogeneous Materials*, Elsevier Science Ltd, North-Holland.
- Parrot, L.J. and Killoh, D.C (1984), “Prediction of cement hydration”, *Chemistry and Chemically-related Properties of Cement*, **35**, 41-53.
- Shah, S.P. (2000), “High performance concrete-workability”, *Strength and Durability, the Hong Kong University of Science and Technology*, Hong Kong.
- Simeonov, P. and Ahmad, S. (1995), “Effect of transition zone on the elastic behavior of cement-based composites”, *Cement Concrete Res.*, **25**(1), 165-176.
- Ulrik Nilsen, A. and Monteiro, P. (1993), “Concrete: a three phase material”, *Cement Concrete Res.*, **23**(1), 147-151.
- Yang, C.C. (1998), “Effect of the transition zone on the elastic moduli of mortar”, *Cement Concrete Res.*, **28**(5), 727-736.
- Yang, C.C. and Su, J.K. (2002), “Approximate migration coefficient of interfacial transition zone and the effect of aggregate content on the migration coefficient of mortar”, *Cement Concrete Res.*, **32**(10), 1559-65.
- Yang, C.C. (2003), “The relationship between charge passed and the chloride concentrations in anode and cathode cells using the accelerated chloride migration test”, *Mater. struct.*, **36**(10), 678-684.
- Yang, C.C. and Liang, C.H. (2009), “The influence of medium–high temperature on the transport properties of concrete by using accelerated chloride migration test”, *Mater. Chem. Phys.*, **114**(2-3), 670-675.